Fermi National Accelerator Laboratory

FERMILAB-Conf-95/175-E
CDF

Quarkonia Production in $p\bar{p}$ Collisions with CDF

G. Bauer
For the CDF Collaboration

Fermi National Accelerator Laboratory
P.O. Box 500, Batavia, Illinois 60510

July 1995

Published Proceedings for the *10th Topical Workshop on Proton-Antiproton Collider Physics*, Fermilab, Batavia, Illinois, May 9-13, 1995

Disclaimer

QUARKONIA PRODUCTION IN $p\bar{p}$-COLLISIONS WITH CDF

CDF Collaboration
Represented by
G. Bauer

Massachusetts Institute of Technology
Cambridge, Massachusetts

The production cross sections for Υ's, ψ's and χ_c's in high energy $p\bar{p}$ collisions have been measured using the CDF detector at Fermilab. Heavy quarkonia production involves a variety of mechanisms, and the data is used to disentangle various components. Large prompt ψ-cross sections were observed, contrary to conventional expectations.

I. INTRODUCTION

The production of $c\bar{c}$ and $b\bar{b}$ bound-states in high energy $p\bar{p}$ collisions is of interest as another testing ground for perturbative QCD. Several mechanisms are expected to contribute. The lowest order process is gluon fusion producing a $Q\bar{Q}$ pair plus a final state gluon, which we refer to as "direct production" (Fig. 1a). An additional process is "fragmentation" (Fig. 1b), where a gluon (or quark) fragments into a $Q\bar{Q}$ pair. This is formally a higher order process, however it was realized a few years ago (1) that fragmentation has a p_T-dependence ($\sim p_T^2/m_Q^2$, where p_T is the transverse momentum of the heavy quark, and m_Q is its mass), and that at high p_T this process can surpass direct production. The observed ψ's are biased to be at high p_T due to the p_T-cutoff of the daughter leptons in the CDF detector; whereas the heavier Υ's can probe low onia p_T. One can thereby probe different kinematic regimes for effects like the importance of fragmentation by comparing Υ's, ψ's, and the p_T-dependence of their production.

The lowest order of both processes result in χ-states. Production of ψ's or Υ's are suppressed by the extra gluon needed to obtain the 1^- spin-parity. Radiative χ-decay was therefore thought to be the dominant source of J/ψ's (2–6) and Υ's (2). This feeddown is not relevant for ψ' as it is above the χ_c's.

There is however an additional source which does feeddown to the ψ', as well as for the J/ψ, and that is B-decay (7). The B-mesons have an appreciable ($\sim 1\%$) branching fraction $B \rightarrow \psi + X$; and with μbarn cross sections this process is a significant source for ψ's. In fact, the traditional view point has been that since the ψ' has only the (suppressed) direct/fragmentation processes, B-decay was likely their dominant source (3,8).

In summary, the traditional wisdom has been that J/ψ's come predominately from χ_c decays, with a substantial fraction from B-decay; whereas the ψ' would be almost completely from B-decay. The majority of the Upsilons would be from χ_b-decays. It is within this framework that prior collider data was viewed, and with the type and quantity of data available, it was a reasonably consistent picture (9,10). A more extensive view of contemporary quarkonia phenomenology can be found elsewhere these proceedings (11).

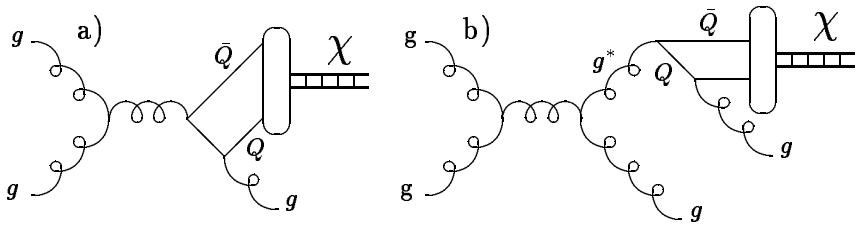

FIG. 1. Example of χ-production by Feynman diagrams for: a) "direct production"; and b) "fragmentation".

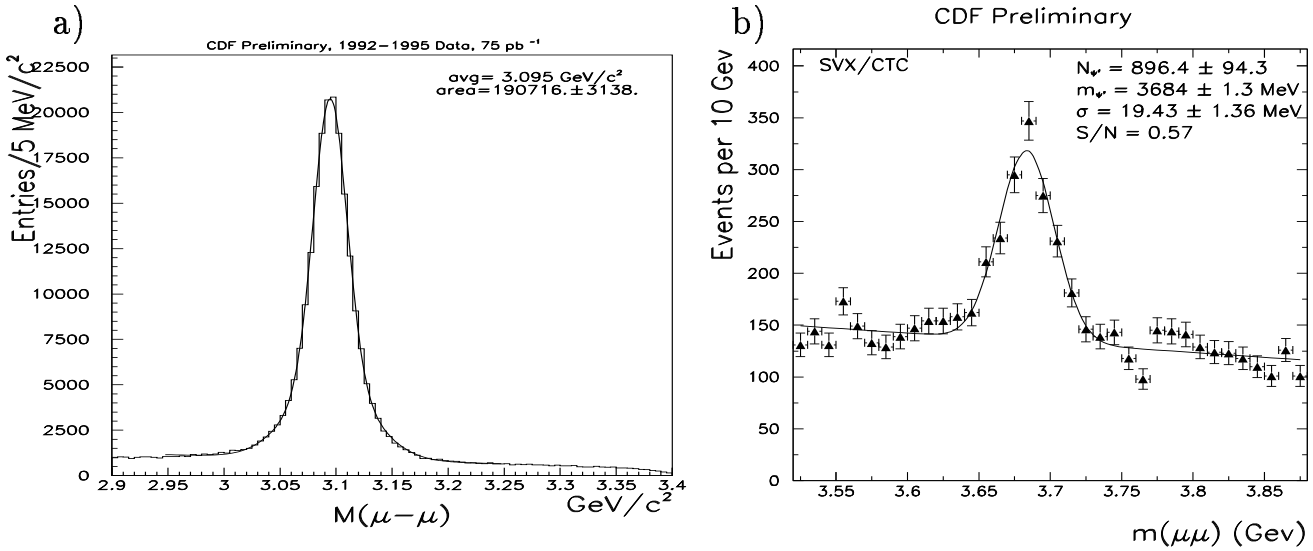

FIG. 2. Dimuon mass distribution around a) the J/ψ for 75 pb^{-1}; and b) the ψ' for 18 pb^{-1}.

II. THE CDF DETECTOR AND DATA SETS

The data presented here are from $p\bar{p}$ collisions at $\sqrt{s}$ of 1.8 TeV collected with the CDF detector, a large general purpose detector composed of a magnetic tracking system, calorimeters, and muon chambers. The detector has been described in detail elsewhere (12); we note here a few salient features. The tracking system is contained in a 1.4 T axial magnetic field, and consists of a 4-layer Si-μvertex detector (13) followed by drift chambers. After the solenoid coil and cryostat is the central electromagnetic calorimeter (Pb-scintillator sandwich with $15^\circ(\phi) \times 0.1(\eta)$ towers). Imbedded in the calorimeter at a depth of 5.9 radiation lengths is a strip chamber to measure shower position. The E.M. calorimeter is followed by an Fe-scintillator hadronic calorimeter which also acts as an absorber for the 4 layers of the Central MUon (CMU) ($\mid \eta \mid < 0.6$, $P_T^{min} \sim 1.4$ GeV/c) drift chambers that follow it. The CMU is followed by an additional 60 cm of steel and another 4 planes of the Central Muon uPgrade (CMP) chambers. Muon coverage is extended to the range $0.6, < \mid \eta \mid < 1.0$ by the Central Muon eXtension (CMX) chambers.

The data are from the 1992-95 collider runs. The analyses are at varying stages, and range from 15 pb^{-1} to 75 pb^{-1} in luminosity. The run is continuing, and the final data sets may reach $\sim$ 150 pb^{-1}. The event selection required a variety of technical quality cuts, and the following kinematic cuts:

- Two opposite sign central muons;
- p_T of the hard muon > 2.8 GeV/c;
- p_T of the soft muon > 2.0 GeV/c;
- $p_T(\mu^+\mu^-) > 4.0$ GeV/c for Psi's, or
  $p_T(\mu^+\mu^-) > 0.5$ GeV/c for Upsilons;
- $\mid \eta \mid < 0.6$ for Psi's, or
  $\mid y \mid < 0.4$ for Upsilons;

and, for the Υ's, at least one muon must also be detected in the CMP.

As an example, Fig. 2a shows the dimuon mass distribution in the vicinity of the J/ψ for $\sim$ 75 pb^{-1}. There are about 180,000 J/ψ's in a narrow peak with very clean background. The signal-to-noise is not as good for the ψ', but as shown in Fig. 2b ($\sim$ 18 pb^{-1}), it is nonetheless a strong signal.

Correcting for acceptance and efficiencies, we can convert the numbers of events into cross sections. The trigger, reconstruction, and cut efficiencies are determined from data. Acceptance due to geometry and kinematics are determined from Monte Carlo simulations. Variations in M.C. parameters are folded into the systematic error estimates.

III. PRODUCTION OF UPSILONS

First, we consider the case of the Upsilons, where the analysis is based on $\sim 17\,\mathrm{pb}^{-1}$. The event selection of the previous section resulted in a sample of about 1200 $\Upsilon(1S)$'s, and several hundred 2S and 3S. Converting the event numbers into cross sections yields:

$$\begin{aligned}
\sigma(p\bar{p} \to \Upsilon(1S) + X, \mid y \mid < 0.4,\, p_T > 0.5\,\mathrm{GeV/c}) &= 23.48 \pm 0.99 \pm 2.80\,\mathrm{nb} \\
\sigma(p\bar{p} \to \Upsilon(2S) + X, \mid y \mid < 0.4,\, p_T > 1.0\,\mathrm{GeV/c}) &= 10.07 \pm 1.01 \pm 1.99\,\mathrm{nb} \\
\sigma(p\bar{p} \to \Upsilon(3S) + X, \mid y \mid < 0.4,\, p_T > 1.0\,\mathrm{GeV/c}) &= 4.79 \pm 0.64 \pm 0.72\,\mathrm{nb}
\end{aligned}$$

where the first error is statistical, and the second is systematic (a convention followed through out this paper when two errors are quoted). The preliminary D0 cross section summed over the three S-states of $58.8 \pm 6.4 \pm 11.3$ nb ($p_T > 0\,\mathrm{GeV/c}$, $\mid y \mid < 0.7$) (14) is consistent with these results.

The statistics is sufficient to also obtain differential cross sections, where the p_T-dependence may be studied. The dimuon mass distribution was broken up into p_T-bins, and fit with a gaussian and linear background. Acceptance and efficiency corrections were applied to obtain differential cross sections, shown in Fig. 3. The vertical error bars are the statistical error added in quadrature with p_T-dependent systematic errors. There remains a common systematic error of 15% (22%) for the 1S (2S) which is not included.

Also shown are leading order QCD calculations (2,15) of the cross section using MRSD0 structure functions (16) with a scale $\mu^2 = p_T^2 + m_\Upsilon^2$. The calculation includes the contribution from the production and radiative decay of $\chi_b(1P)$ and $\chi_b(2P)$ states, but not from the undiscovered $\chi_b(3P)$.

The data is higher than the theory in all cases. For the 1S and 2S it is about a factor of 3 higher, but for the 3S the data is about 10 times higher. The calculation predicts that the χ_b's are the dominant source of Υ's, and a natural explanation of the large discrepancy for the 3S is likely that the $\chi_b(3P)$ does indeed exist with a large radiative decay to the $\Upsilon(3S)$. The addition of fragmentation (17) or other new mechanisms (18,19) may reduce the disparity of the theory for these three states.

IV. PRODUCTION OF PSI'S

A. $\psi(2S)$

Next consider the case of the $\psi(2S)$, where analysis of $18\,\mathrm{pb}^{-1}$ of data (20) resulted in a total cross section of $0.721 \pm 0.058 \pm 0.072$ nb ($\mid \eta \mid < 0.6$, $p_T > 4.0$ GeV/c).

The nominal expectation (3,8) for the $\psi(2S)$ had been that the contribution from fusion and fragmentation should be small; and there is no feeddown from χ_c states. So by far the dominant source would be expected from B-decay.

The problem is to distinguish between prompt production and B-decay. Previously, it was difficult to experimentally separate the prompt and B-decay sources, and the theoretical prejudice was sometimes used to measure B cross sections by *assuming* the $\psi(2S)$ was virtually all B-decay (9).

The Si-μvertex detector (13) is a powerful tool which can make this distinction due to the relatively long lifetime of the B. Selecting the events where the J/ψ has two muons reconstructed in the SVX permits a meaningful measurement of a decay length. However, as this is not an exclusive B-reconstruction, the $\beta\gamma$ factor needed to transform the decay length into a proper lifetime is not known. An average correction factor, F_{corr} is determined from Monte Carlo to convert the transverse decay length (l_{xy}) into a "pseudo-cτ" ($c\tau_{pseudo}$) (21):

$$c\tau_{pseudo} = \frac{l_{xy}}{(p_T^\psi / M^\psi) \cdot F_{corr}}\,; \quad l_{xy} = \vec{x} \cdot \vec{p}_T^{\,\psi} / p_T^\psi$$

where $\vec{x}$ is the spatial displacement of the decay vertex.

The pseudo-cτ distribution is then fit for three components: prompt (gaussian shape), B-decay (exponential smeared by resolution), and background (shape determined from $\psi(2S)$-sidebands). Figure 4 shows the pseudo-cτ distribution along with the decomposition that results from the fit; overall, $22.8 \pm 3.8\%$ are from B-decay, far from being dominant. The statistics are sufficient that this decomposition can be done in several p_T bins, as is given in Table 1.

The fraction of $\psi(2S)$'s coming from B-decay can be used along with the total to determine the differential cross section for $B \to \psi(2S) + X$. This measurement is shown in Fig 5a along with NLO QCD calculations (22) of B-production/decay. The different curves are for various choices of the μ-scale ($+\delta Br$ signifies setting the branching ratio 1σ higher). The theory is in fairly good agreement with the data.

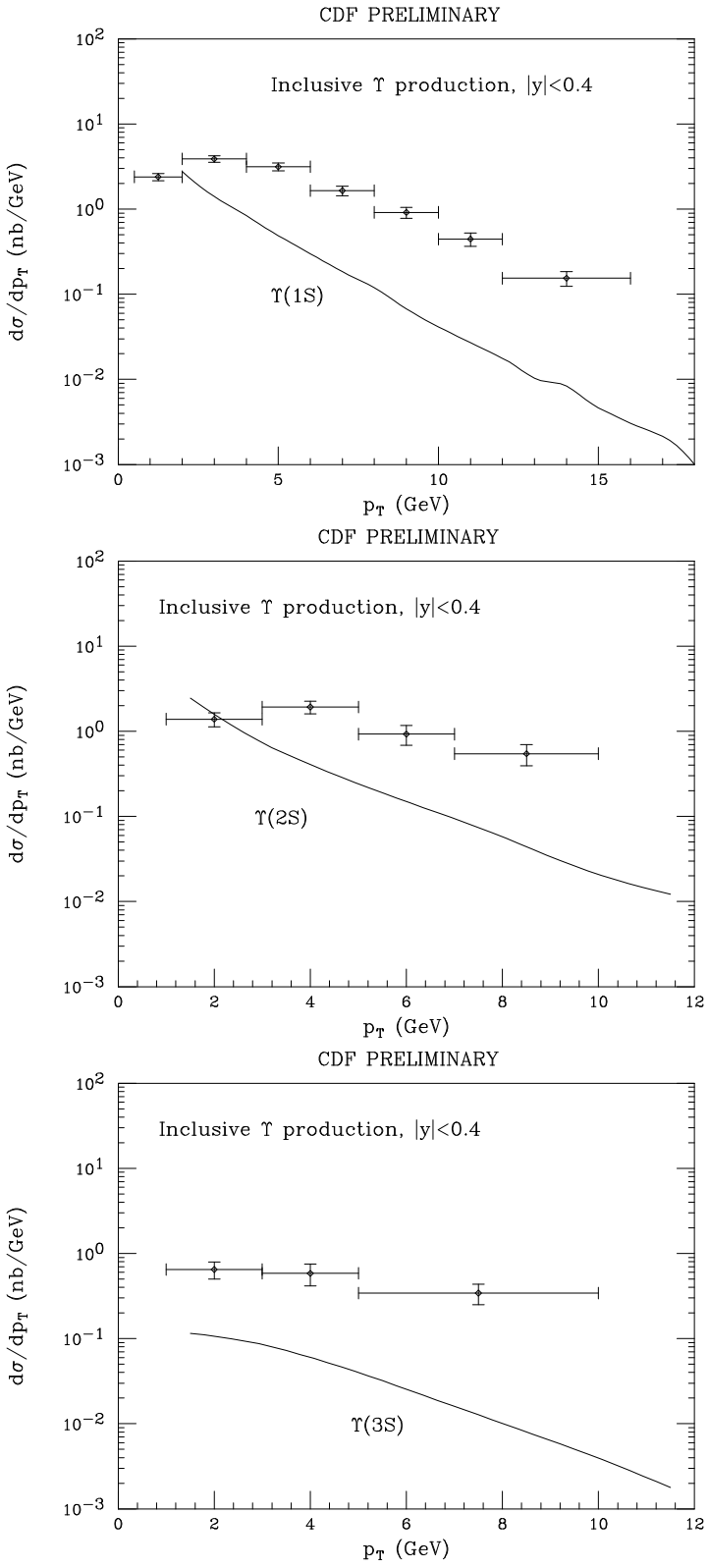

FIG. 3. Differential Upsilon cross sections together with leading order QCD calculations.

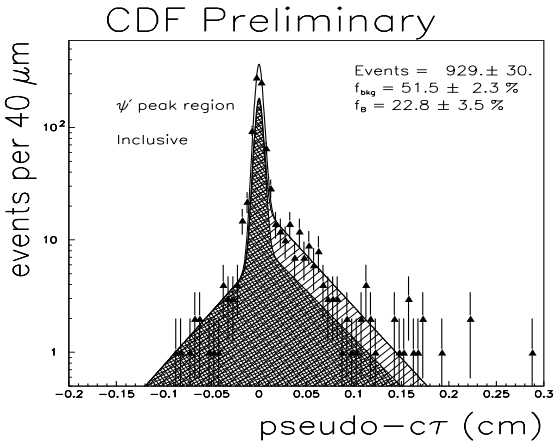

FIG. 4. Pseudo-cτ distribution for $\psi(2S)$ decomposed into prompt (unshaded), B-decay (light cross hatch), and background components (dark shading).

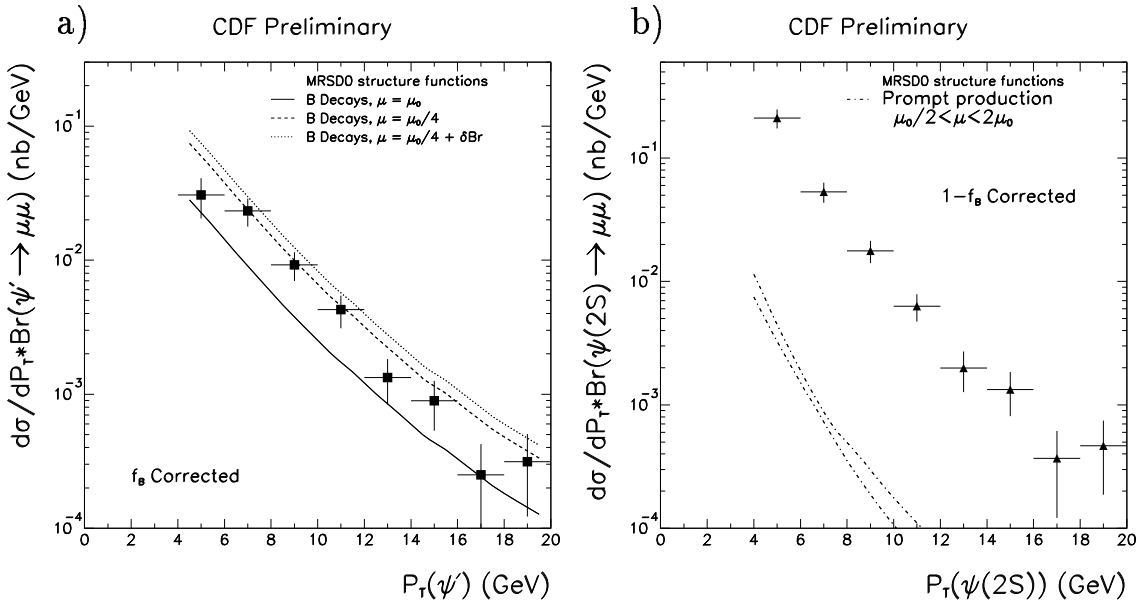

FIG. 5. $\psi(2S)$ differential cross section: a) B-component with NLO QCD calculation (22) (MRSD0 structure functions, $\mu_0 = \sqrt{M_b^2 + p_T^2}$); and b) prompt component with QCD calculation (6) based on fusion and fragmentation processes.

TABLE 1. Psi Fractional Decompositions: summary of the the fraction of ψ's that originate from B-decay, and, for the J/ψ, from radiative χ_c-decay, in p_T-bins of the ψ. The χ-fraction is given for both the case where $B \to \chi + X$ contributes (3rd column), and where B's are removed and only the prompt χ_c-production is considered (4th column). A single quoted error is statistical and systematic combined, dual errors are statistical followed by systematic.

	$\psi(1S)$			$\psi(2S)$
$p_T(\psi)$ (GeV/c)	B-Frac. (%)	χ-Frac. (%)	χ-Frac. (B's Subtr.)(%)	B-Frac. (%)
> 4.0	19.6 ± 1.5	$28.3 \pm 1.6 \pm 6.8$	$32.3 \pm 2.0 \pm 8.5$	22.8 ± 3.8
4 - 5	13.3 ± 1.0	$30.2 \pm 2.6 \pm 7.2$	$33.3 \pm 3.1 \pm 8.5$	12.3 ± 4.9
5 - 6	15.9 ± 1.2			
6 - 7	21.0 ± 1.7	$26.8 \pm 2.2 \pm 6.4$	$31.1 \pm 2.9 \pm 8.3$	29.5 ± 7.0
7 - 8	25.2 ± 2.1			
8 - 9	25.2 ± 2.2	$22.4 \pm 2.8 \pm 5.4$	$26.0 \pm 3.8 \pm 7.4$	
9 - 10	26.9 ± 2.5			
10 - 11	34.3 ± 3.3	$22.0 \pm 2.9 \pm 5.3$	$27.0 \pm 4.5 \pm 8.0$	39.3 ± 7.9
11 - 12	31.0 ± 3.5			
12 - 13	32.4 ± 4.1			
13 - 14	42.1 ± 5.7			
14 - 15	27.6 ± 5.0			
15 - 20	–	–	–	

On the other hand, the prompt component is shown in Fig 5b. There is a very large discrepancy between the data and the theoretical calculation (6), about 50 times. The failure of the QCD model (6,17) – which includes fragmentation as well as gluon fusion processes – has prompted a number of proposals. These suggestions generally fall into two classes: 1) the existence of new charmonium states above the the $D\bar{D}$-threshold, but whose decay to open charm is suppressed by quantum numbers (23); or 2) a new production mechanism, such as the "color-octet" mechanism in which a color-octet is formed in *addition* to the usual color-singlet state (18,19). The case for the latter possibility was advocated at this workshop (11).

B. $\psi(1S)$

– B-Decay vs. Prompt Production –

The J/ψ is the most complex case: the prompt and B-components are present as before, but one must also consider the contribution from radiative χ_c-decay which were thought to dominate (2–6). The total cross section measurement from $15\,\mathrm{pb}^{-1}$ of data yielded $29.1 \pm 0.19\,^{+3.05}_{-2.84}\,\mathrm{nb}$ ($|\,\eta\,| < 0.6, p_T > 4$ GeV/c). The preliminary D0 cross section $2.00 \pm 0.17 \pm 0.57\,\mathrm{nb}$ ($p_T > 8\,GeV/c, |\,\eta\,| < 0.6$) (14), although over a smaller kinematic range, is in agreement.

The prompt and B-decay components are separated as before, using the pseudo-cτ distributions (20). The B-fraction is found to be about 20% (Table 1), similar to $\psi(2S)$. The corresponding cross sections are shown in Fig. 6 along with QCD calculations. The contribution from B-decays (22) is fairly well described by the data.[1] However the prompt component is again underestimated by the theory (6), although not as dramatically as with the $\psi(2S)$.

– $\chi_c \to J/\psi\,\gamma$ –

Next, we address the issue of the χ_c-contribution where new results have just become available. For this, J/ψ events are selected ($20\ \mathrm{pb}^{-1}$) which have an electromagnetic calorimeter deposition greater than 1 GeV with no charged tracks pointing to the respective tower. The E.M. strip chamber is used to accurately measure the shower position, which is used along with the interaction vertex to define the photon direction. This direction and the calorimeter energy measurement are combined with the muon track information to compute the $J/\psi\gamma$ mass. The mass difference between

[1] The data is systematically a little higher than the theory curve, but this is also the case for the $\psi(2S)$. The agreement is improved if the μ-scale is lowered to $\mu_0/4$.

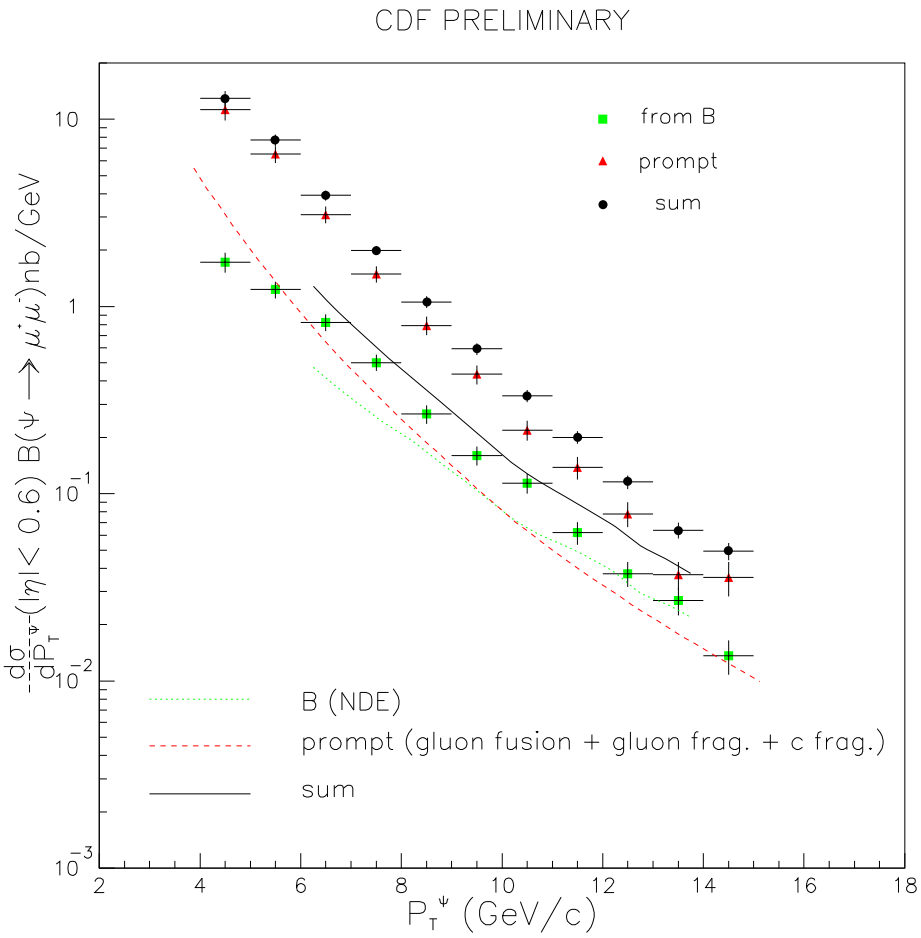

FIG. 6. J/ψ differential cross section (circles, solid line), and its subcomponents of prompt (triangles, dashed line) and B-decay ($\times$'s, dotted line).

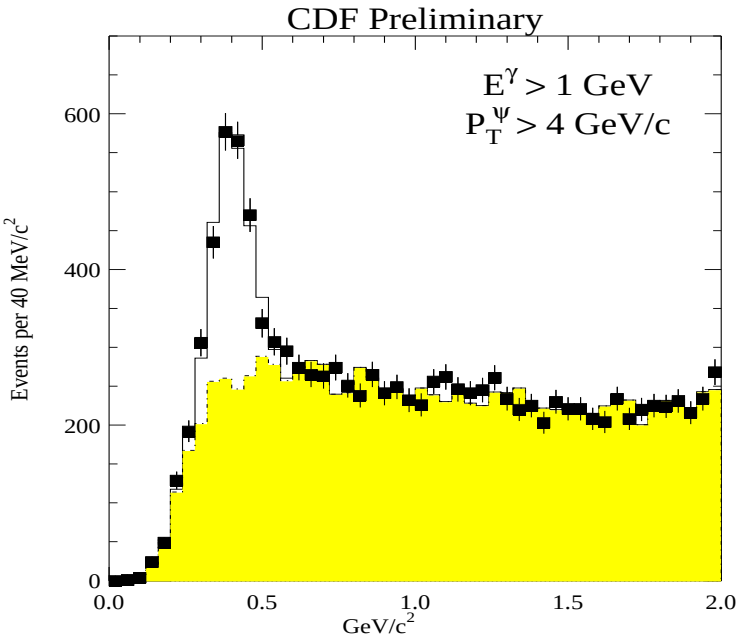

FIG. 7. The mass difference between the $\mu^+\mu^-\gamma$ and $\mu^+\mu^-$ systems. A clear χ_c peak is present in the data (black squares); with the background estimation indicated by the shaded histogram. A fit of a gaussian signal plus the background histogram is shown by the solid line histogram.

the $J/\psi\gamma$ and J/ψ systems is plotted in Fig. 7, showing a clear peak of over a thousand χ_c candidates. The width of the peak is about 60 MeV/c^2, too large to distinguish the χ_{c1} and χ_{c2} ($\Delta M_{\chi_2-\chi_1}$ of 45.7 MeV/c^2).

Determination of the signal of course requires the appropriate background subtraction, which in this case is a delicate matter with the signal appearing at threshold. The background is modelled in the following way. We start with the actual J/ψ events, randomly select and remove a charged track, and use a Monte Carlo to replace it by a π^0, η or a K_s^0 [2]. The Monte Carlo decays the meson into photons, and simulates the detector response. These hybrid data-simulation events are then analyzed in the same fashion as the real data, providing the shape of the background. As a check of the veracity of this background model, it was compared to the ΔM distribution obtained by using $\mu^+\mu^-$-pairs in the J/ψ-*sidebands*. The two agree very well (within statistics) in all p_T-bins.

The number of signal events is extracted by fitting the data to the sum of a gaussian and the background shape determined above. For $p_T > 4.0$ GeV/c we find $28.3 \pm 1.6 \pm 6.8\%$ of the J/ψ's are from χ's. The fractions broken down into p_T-bins is given in Table 1. These results are lower than, but consistent with, the previous CDF χ-fraction of $45.0 \pm 5.5 \pm 15\%$ ($p_T^{\psi} > 6.0$ GeV/c) based on 2.6 pb^{-1} of data (10); and also agree with a preliminary fraction from D0: $30 \pm 7 \pm 5\%$ ($p_T^{\psi} > 8.0$ GeV/c, $|\eta| < 0.6$) (14).

There is of course a residual contribution from B-decays: $B \rightarrow \chi_c X$ has a branching ratio of ~ 0.3 %. We can repeat our earlier procedures for obtaining B-contributions via the pseudo-cτ distribution. However given the limited statistics, a more precise result is obtained by a subtraction based on the measured branching ratios (24) in conjunction with our previous J/ψ and $B \rightarrow J/\psi X$ cross section measurements. The prompt J/ψ and $\chi \rightarrow J/\psi\gamma$ cross-sections *without* any B-contribution are shown in Fig. 8. The fractional results are also given in Table 1. It is clear from these results, and contrary to conventional wisdom, that prompt J/ψ-production is *not* dominated by χ_c production and decay. There is a large prompt component as there was for the $\psi(2S)$, although the magnitude of the discrepancy is smaller for the J/ψ.

As was noted earlier, this χ-analysis has insufficient resolution to distinguish the two χ_c-states. A complimentary analysis can be done, now updated to 75 pb^{-1}, which utilizes the excellent resolution of the tracking system – albeit at

[2] This was done in the ratio $\pi^0 : \eta : K_s^0 :: 0.4 : 0.2 : 0.1$. The result was found not to be very sensitive these ratios, and the variation is included in the systematic error.

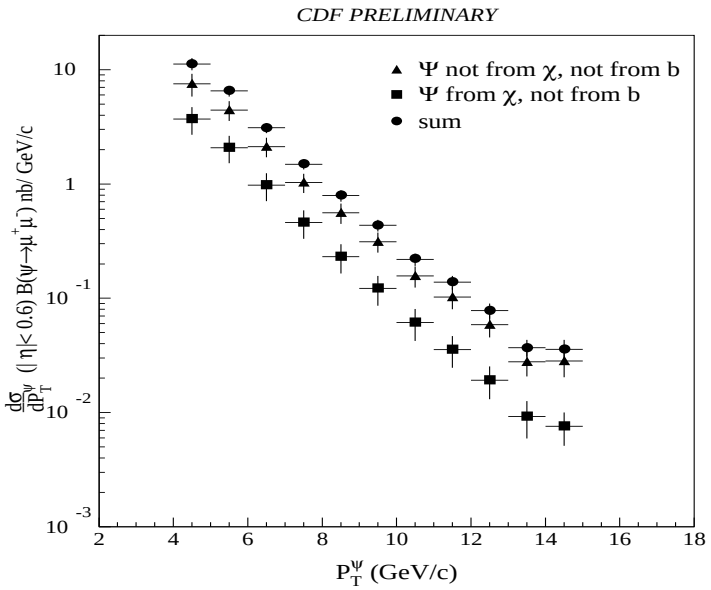

FIG. 8. The differential cross section of J/ψ's showing the separate subcomponents for radiative χ_c-decay with the B-decay contribution removed (squares), the non-χ_c prompt (triangles), and the sum (circles).

low efficiency – to reconstruct photons by conversion. Events are selected[3] by reconstructing a photon conversion with p_T greater than 1.0 GeV/c, and conversion vertex displaced from the primary by more than 1.0 cm in the transverse plane. Prompt candidates are selected by requiring the J/ψ pseudo-$c\tau$ to be less than 100 μm. The resulting $J/\psi\gamma$ mass distribution is shown in Fig. 9. While relatively low statistics, the χ_{c1} and χ_{c2} states are readily identifiable and cleanly separated. The event rates, corrected for acceptance, can be used to obtain the relative cross sections:

$$\frac{\sigma(\chi_{c2})}{\sigma(\chi_{c1})+\sigma(\chi_{c2})} = 0.47 \pm 0.08\,(stat.)\,0.02 \pm (sys.)$$

which is compatible with theoretical expectations (4).

SUMMARY

We have measured production cross sections for the Υ's, ψ's, and χ_c's in high energy $p\bar{p}$ collisions. This data has helped provide insight into the variety of mechanisms involved in heavy quarkonia production.

The Υ cross sections for the 1S and 2S were found to be $\sim 3\times$ larger than leading order QCD, and the 3S was $\sim 10\times$ larger. The substantial disagreement of the 3S may plausibly be accounted for by the radiative decay of the (unobserved) $\chi_b(3P)$, which was not included in the calculation.

The ψ's on the other hand have more complex production mechanisms, and experimentally are biased towards high p_T where fragmentation production becomes more important. Even so, inclusion of fragmentation is unable to account for the data. The case of the $\psi(2S)$ is quite striking where the disagreement is a factor of 50; and has initiated considerable theoretical speculation. One proposal, invoking "color-octet" diagrams, offers the prospect of addressing these discrepancies, for the ψ' as well as for the large non-χ J/ψ cross section and the excess Υ's. This data is in fact now being used to extract the unknown matrix elements in the color-octet model (11,19).

In the near future the analyses will be extended to larger data sets with which studies of increasing precision may be made of quarkonia production at the Tevatron.

[3]This selection differed slightly: p_T^μ cuts lowered to 1.8 and 2.8 GeV/c.

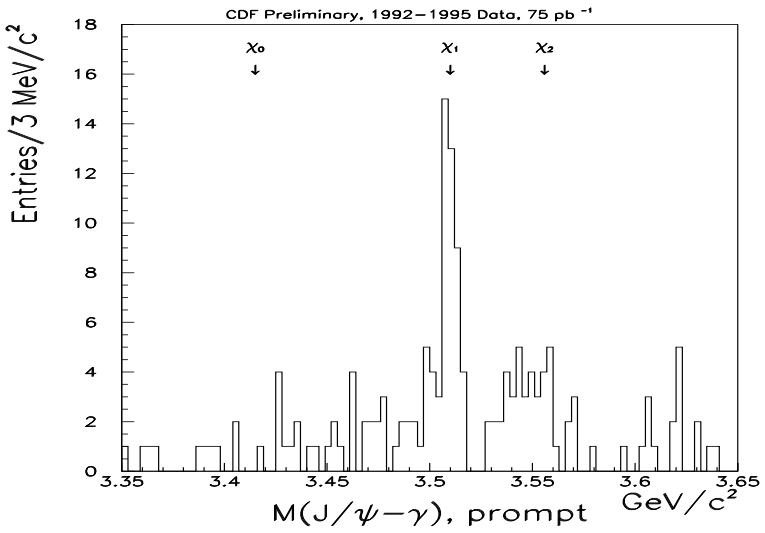

FIG. 9. The $J/\psi - \gamma$ mass distribution as measured by the tracking system via photon conversions.

ACKNOWLEDGEMENTS

Commendations go to the FNAL Accelerator Division for the impressive improvements of the Tevatron collider, without which these results would hardly have been possible. I wish to thank my fellow CDF collaborators for the pleasure of representing them at this workshop. And a special thanks go to T. Daniels, P. Lukens, V. Papadimitriou, and P. Sphicas whose assistance and insight greatly aided this presentation.

REFERENCES

1. E. Braaten and T.C. Yuan, Phys. Rev. Lett. **71** 1673 (1993).
2. R. Baier and R. Rückl, Phys. Lett. **B102**, 364 (1981);
   Nucl. Phys. **B208**, 381 (1982);
   Z. Phys. C **19**, 251 (1983).
3. E.W.N. Glover, F. Halzen, and A.D. Martin, Phys. Lett. **B185**, 441 (1987).
4. E.W.N. Glover, A.D. Martin, W.J. Stirling, Z. Phys. **C38**, 473 (1988).
5. M. Cacciari and M. Greco, Phys. Rev. Lett. **73**, 1586 (1994).
6. E. Braaten *et al.* Phys. Lett. **B333** 548 (1994).
7. H. Fritzsch, Phys. Lett. **B86** 164, 343 (1979).
8. M.L. Mangano, Z. Phys. C **58**, 651 (1993).
9. UA1 Collaboration, C. Albajar *et al.*, Phys. Lett. **B213**, 405 (1988);
   UA1 Collaboration, C. Albajar *et al.*, Phys. Lett. **B256**, 112 (1991);
   CDF Collaboration, F. Abe *et al.*, Phys. Rev. Lett. **69**, 3704 (1992).
10. CDF Collaboration, F. Abe *et al.*, Phys. Rev. Lett. **71**, 2537 (1993)
11. M. Mangano, these proceedings.
12. CDF Collaboration, F. Abe *et al.*, Nucl. Instrum. Methods **A271**, 387 (1988).
13. SVX: D. Amidei *et al.*, Nucl. Instrum. Methods **A350** 73, (1994);
    SVX′: P. Azzi *et al.*, Nucl. Instrum. Methods **A360** 137, (1995).
14. D0 Collaboration, K. Bazizi, these proceedings.
15. M. Mangano, private communication.
16. A.D. Martin, R.G. Roberts, and W.J. Stirling, Phys. Lett. **B306**, 145 (1993).
17. D.P. Roy and K. Sridhar, Phys. Lett. **B339**, 141 (1994).
18. E. Braaten and S. Fleming, Phys. Rev. Lett. **74**, 3327 (1995).
19. P. Cho and A.K. Leibovich, CALT-68-1988 (1995).

20. More technical details of this analysis may be found in:
CDF Collaboration, Fermilab-Conf-94/136-E (1994).
21. This is a standard technique for non-exclusive analysis, for more details see:
CDF Collaboration, F. Abe *et al.*, Phys. Rev. Lett. **71**, 3421 (1993).
22. P. Nason, S. Dawson, and R. Ellis, Nucl. Phys. **B303** 607, (1988); **B327** 49, (1989); **B335** 260, (1990).
23. P. Cho, S. Trivedi, and M. Wise, Phys. Rev. **D51**, 2039 (1995);
F.E. Close, Phys. Lett. **B342**, 369 (1995);
D.P. Roy and K. Sridhar, Phys. Lett. **B345**, 537 (1995);
P. Cho and M. Wise, Phys. Lett. **B346**, 129 (1995).
24. $B(B \to J/\psi + X) = 1.12 \pm 0.04 \pm 0.06\%$, $B(B \to \chi_{c1} + X) = 0.40 \pm 0.06 \pm 0.04\%$, $B(B \to \chi_{c2} + X) = 0.25 \pm 0.10 \pm 0.03\%$, from: R. Balest *et al.*, "Inclusive Decays of B Mesons to Charmonium", CLNS 94/1315.